

“Sun” to  $\approx 10^6$  is required; this is not possible without special devices — modal filters — that equalize the wavefronts arriving from the two telescopes.

Currently, modal filters in the  $\approx 10\text{-}\mu\text{m}$  spectral range are implemented as single-mode fibers. Using semiconductor technology, single-mode waveguides for

use as modal filters were fabricated. Two designs were implemented: one using an InGaAs waveguide layer matched to an InP substrate, and one using InAlAs matched to an InP substrate. Photon Design software was used to design the waveguides, with the main feature all designs being single-mode operation in the

10.5- to 17- $\mu\text{m}$  spectral range. Preliminary results show that the filter’s rejection ratio is 26 dB

*This work was done by Alexander Ksendzov, Daniel R MacDonald, and Alexander Soibel of Caltech for NASA’s Jet Propulsion Laboratory. For more information, contact iaoffice@jpl.nasa.gov. NPO-44457*

## Mo<sub>3</sub>Sb<sub>7-x</sub>Te<sub>x</sub> for Thermoelectric Power Generation

These materials could be segmented with lower-temperature thermoelectric materials.

NASA’s Jet Propulsion Laboratory, Pasadena, California

Compounds having compositions of Mo<sub>3</sub>Sb<sub>7-x</sub>Te<sub>x</sub> (where  $x = 1.5$  or  $1.6$ ) have been investigated as candidate thermoelectric materials. These compounds are members of a class of semiconductors that includes previously known thermoelectric materials. All of these compounds have complex crystalline and electronic structures. Through selection of chemical compositions and processing conditions, it may be possible to alter the structures to enhance or optimize thermoelectric properties.

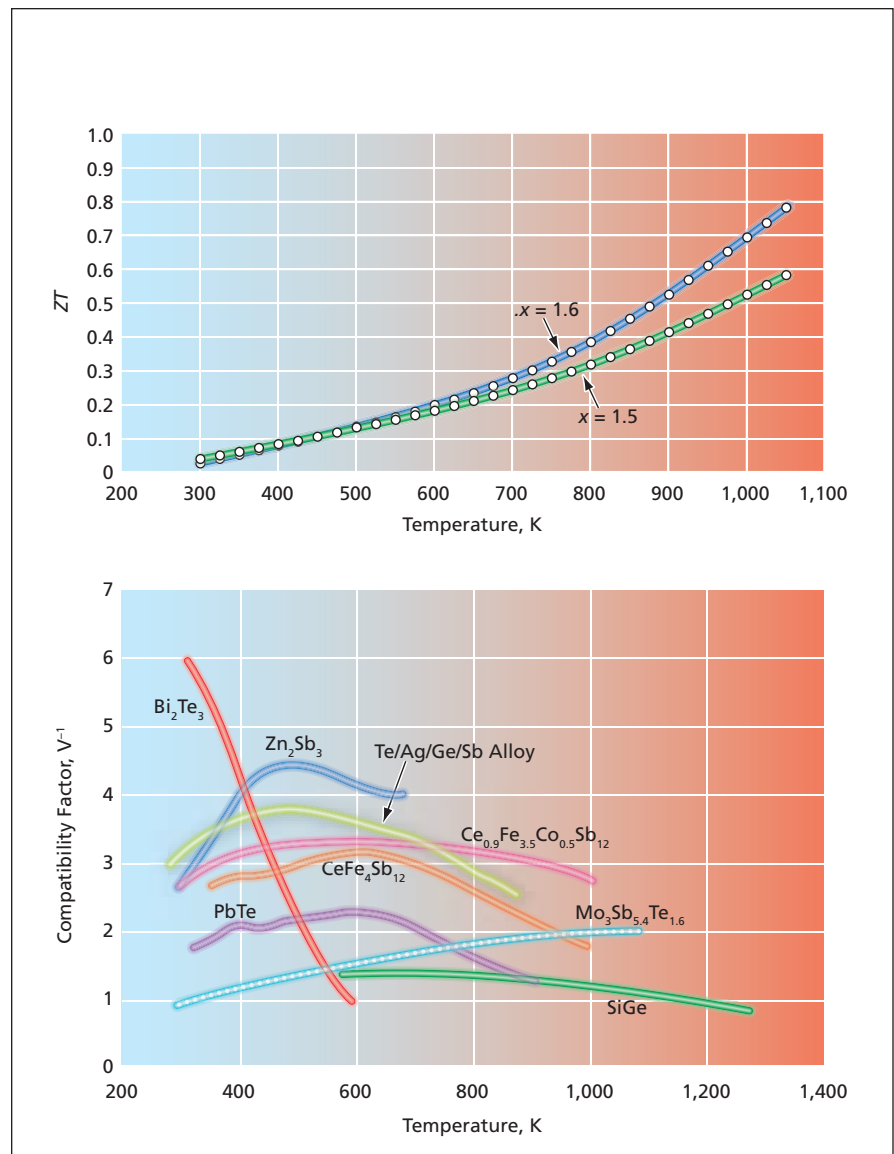
For the investigation, each specimen of Mo<sub>3</sub>Sb<sub>7-x</sub>Te<sub>x</sub> was synthesized as follows:

1. A mixture of specified proportions of Mo, Sb, and Te powders was heated for 7 days at a temperature of 750 °C in a covered boron nitride crucible in an evacuated, sealed fused silica ampule.
2. The chemical reactions were quenched in cold water.
3. In an argon atmosphere, the crucible was opened and the reacted powder mixture was ground in an agate mortar.
4. The powder was annealed by again heating it as in step 1.
5. The powder was formed into a dense cylindrical specimen by uniaxial pressing in a high-density graphite die for 1 hour at a pressure of about 20 kpsi ( $\approx 138$  MPa) and temperature of 873 °C in an argon atmosphere.

The traditional thermoelectric figure of merit,  $Z$ , is defined by the equation  $Z = \alpha^2 / \rho \kappa$ , where  $\alpha$  is the Seebeck coefficient,  $\rho$  is the electrical resistivity, and  $\kappa$  is the thermal conductivity. Often, in current usage, the term “thermoelectric figure of merit” signifies the dimensionless product  $ZT$ , where  $T$  is the absolute temperature. The thermoelectric compatibility factor,  $s$ , is defined by the equation  $s = [(1 + ZT)^{1/2} - 1] / \alpha T$ . For maximum efficiency,  $s$  should not change with temper-

ature, both within a single material, and throughout a segmented thermoelectric-generator leg, the segments of which are made of different materials.

Values of  $ZT$  and  $s$  were calculated from measurements of the pertinent physical properties of Mo<sub>3</sub>Sb<sub>7-x</sub>Te<sub>x</sub> specimens as functions at various tem-



Thermoelectric Figures of Merit and compatibility factors of Mo<sub>3</sub>Sb<sub>7-x</sub>Te<sub>x</sub> and other compounds were determined as functions of temperature.

peratures, and the  $s$  values of  $\text{Mo}_3\text{Sb}_{5.4}\text{Te}_{1.6}$  were compared with those of other state-of-the-art thermoelectric materials (see figure). The  $ZT$  values of both  $\text{Mo}_3\text{Sb}_{5.5}\text{Te}_{1.5}$  and  $\text{Mo}_3\text{Sb}_{5.4}\text{Te}_{1.6}$  were found to increase with temperature up to 1,050 K, which is just below the decomposition temperature. The fact that  $ZT$  for  $x = 1.6$  exceeds that for  $x = 1.5$  might be taken as a hint that one could increase  $ZT$  by increasing  $x$ , except for the observation

that attempts to synthesize  $\text{Mo}_3\text{Sb}_{7-x}\text{Te}_x$  having  $x > 1.6$  resulted in specimens that appeared to be multiphase. Hence, other approaches to doping may be more promising.

The  $s$  value of  $\text{Mo}_3\text{Sb}_{5.4}\text{Te}_{1.6}$  was found to increase from about  $1 \text{ V}^{-1}$  at 300 K (room temperature) to about  $2 \text{ V}^{-1}$  at 1,000 K. This doubling of  $s$  indicates poor self-compatibility of  $\text{Mo}_3\text{Sb}_{5.4}\text{Te}_{1.6}$  over the affected temperature range. However,  $\text{Mo}_3\text{Sb}_{5.4}\text{Te}_{1.6}$

could be suitable for segmentation: for example, a  $\text{Mo}_3\text{Sb}_{5.4}\text{Te}_{1.6}$  segment (which can withstand a temperature  $> 800 \text{ K}$ ) could be joined to a lower-temperature PbTe segment at an interface temperature at or slightly below 800 K, where their  $s$  values are equal.

*This work was done by G. Jeffrey Snyder, Frank S. Gascoin, and Julia Rasmussen of Caltech for NASA's Jet Propulsion Laboratory. For more information, contact [iaoffice@jpl.nasa.gov](mailto:iaoffice@jpl.nasa.gov). NPO-43862*

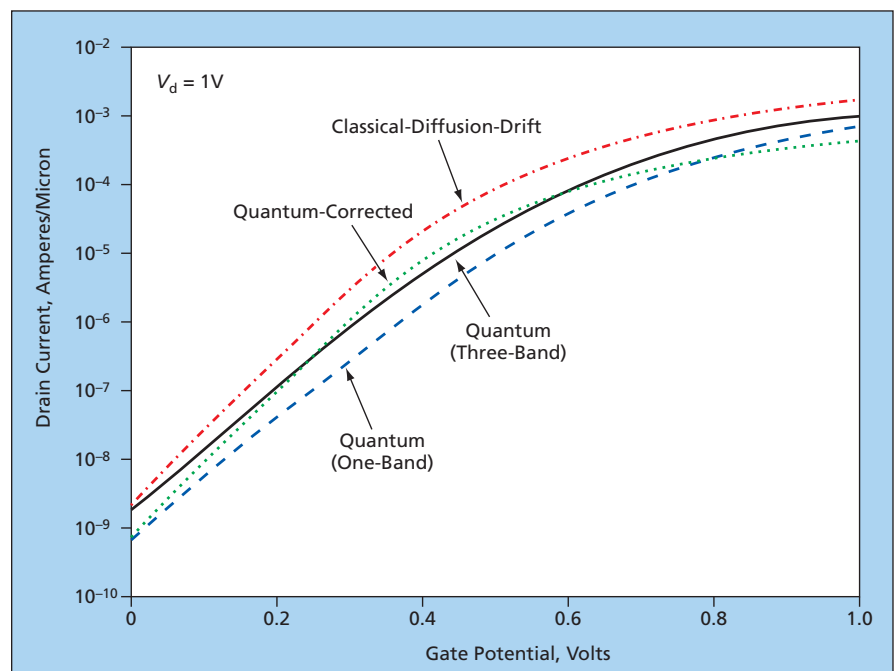
## Two-Dimensional Quantum Model of a Nanotransistor

Quantum effects that become important at the nanoscale are taken into account.

Ames Research Center, Moffett Field, California

A mathematical model, and software to implement the model, have been devised to enable numerical simulation of the transport of electric charge in, and the resulting electrical performance characteristics of, a nanotransistor [in particular, a metal oxide/semiconductor field-effect transistor (MOSFET) having a channel length of the order of tens of nanometers] in which the overall device geometry, including the doping profiles and the injection of charge from the source, gate, and drain contacts, are approximated as being two-dimensional. The model and software constitute a computational framework for quantitatively exploring such device-physics issues as those of source-drain and gate leakage currents, drain-induced barrier lowering, and threshold voltage shift due to quantization. The model and software can also be used as means of studying the accuracy of quantum corrections to other semiclassical models.

The present model accounts for two quantum effects that become increasingly important as channel length decreases toward the nanometer range: quantization of the inversion layer and ballistic transport of electrons across the channel. Heretofore, some quantum effects in nanotransistors have been analyzed qualitatively by use of simple one-dimensional ballistic models, but two-dimensional models are necessary for obtaining quantitative results. Central to any quantum-mechanical approach to modeling of charge transport is the self-consistent solution of a wave equation to describe the quantum-mechanical aspect of the transport, Poisson's equation, and equations for statistics of the particle ensemble.



**Drain Current Versus Gate Potential** in a conceptual 25-nm-gate-length MOSFET commonly used as an example for testing MOSFET-simulating software was calculated by means of a three-band and a one-band version of the present quantum-based model. For comparison, the plot also shows results from a classical diffusion-drift model and a quantum-corrected model embodied in a commercial MOSFET-simulation computer program. A drain bias of 1 V and a gate oxide thickness of 1.5 nm were used in the simulations.

Non-equilibrium Green's function (NEGF) formalisms have been successful in modeling steady-state transport in a variety of one-dimensional semiconductor structures. The present model for the two-dimensional case includes the NEGF equations, which are solved self-consistently with Poisson's equation. At the time of this work, this was the most accurate full quantum model yet applied to simulation of two-dimensional semiconductor devices. Open boundary conditions (in which the nar-

row channel region opens into broad source, gate, and drain regions) and tunneling through oxide are treated on an equal footing. Interactions between electrons and phonons are taken into account, causing the modeled transport to deviate from ballistic in a realistic manner. Electrons in the wave-vector-space ellipsoids of the conduction band are treated within the anisotropic-effective-mass approximation.

Self-consistent solution of the Poisson and NEGF equations is computa-